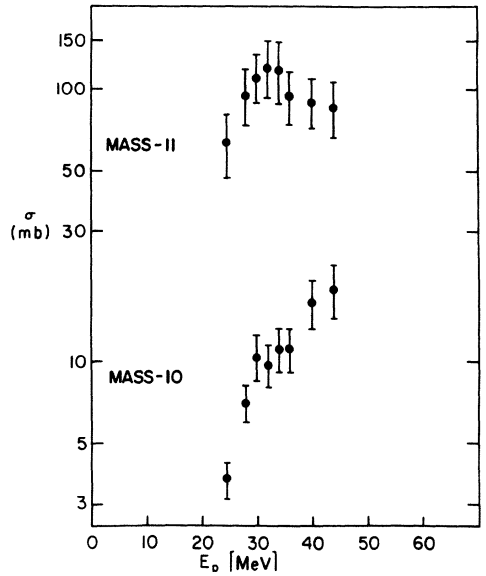

FIG. 2. Cross sections for production of mass-10 and mass-11 isobars by proton-induced reactions in ^{12}C.

duction cross section is significant only for proton energies between 15 and 50 MeV. The cross sections of Fig. 2 show that the production of ^{11}B from ^{12}C considerably exceeds that of ^{10}B under such conditions. The target ^{14}N will also serve as a prolific source of ^{11}B via the low-threshold reaction $^{14}N(p, \alpha)^{11}C$. The low-energy $^{11}B/^{10}B$ ratio for ^{16}O is as yet unknown, but has a value of 2.3 at 135 MeV,[7] in agreement with calculations.[3] These results are consistent with the view of Bernas et al.[3] that the observed $^{11}B/^{10}B$ ratio is the formation ratio, and that the spallation occurs in the stellar atmosphere. Measurements of the ^{10}B and ^{11}B production from ^{14}N and ^{16}O in the threshold region are currently under way in this laboratory.

†Work supported in part by the National Science Foundation.

[1]W. A. Fowler, J. L. Greenstein, and F. Hoyle, Geophys. J. Roy. Astron. Soc. 6, 148 (1962).

[2]D. S. Burnett, W. A. Fowler, and F. Hoyle, Geochim. Cosmochim. Acta 29, 1209 (1965).

[3]R. Bernas, E. Gradsztajn, H. Reeves, and E. Shatzman, Ann. Phys. (N.Y.) 44, 426 (1967).

[4]Although ^{10}Be could be considered stable with its half-life of 2.7×10^6 yr, its production rate is expected to be negligible compared with the total mass-10 yield [Ref. 3; J. Audouze, M. Epherre, and H. Reeves, in High-Energy Nuclear Reactions in Astrophysics, edited by B. S. P. Shen (W. A. Benjamin, Inc., New York, 1967), p. 255; E. Gradsztajn, ibid., p. 247].

[5]M. Shima, J. Geophys. Res. 67, 4251 (1962); D. Krankowsky and O. Muller, Geochim. Cosmochim. Acta 28, 1625 (1964).

[6]J. A. Simpson, private communication.

[7]F. Yiou, M. Basil, J. Dufaure deCitres, P. Fontes, E. Gradsztajn, and R. Bernas, Phys. Rev. 166, 968 (1968).

OBSERVATIONS OF A_1^-, A_2^- AND HIGHER MASS BOSONS PRODUCED NEAR 180° IN $\pi^- p \to p$ (MISSING MASS)$^-$ AT 16 GeV/c*

E. W. Anderson, E. J. Bleser,† H. R. Blieden, G. B. Collins, D. Garelick, J. Menes, and F. Turkot
Brookhaven National Laboratory, Upton, New York 11973

and

D. Birnbaum, R. M. Edelstein, N. C. Hien,‡ T. J. McMahon,§ J. Mucci, and J. Russ
Carnegie-Mellon University, Pittsburgh, Pennsylvania

(Received 9 May 1969)

We report observations of A_1^-, A_2^-, and higher mass bosons produced near 180° in $\pi^- p \to pB^-$ at 16 GeV/c, where B^- denotes missing mass with negative charge. Differential cross sections for pA_1^- and pA_2^- final states are given. Data obtained in the mass range $1.40 \leq M_{B^-} \leq 2.66$ GeV are presented and compared with existing evidence for high mass bosons produced near 0°.

We report here the first detailed search for the production of high-mass bosons ($M_{B^-} > 1.0$ GeV) at small u (i.e., near 180°). This experiment, performed at the Brookhaven National Laboratory alternating-gradient synchrotron (AGS), studied reactions of the type

$$\pi_{(1)}^- + p_{(2)} \to p_{(3)} + B_{(4)}^- \qquad (1)$$

at an incident beam momentum of 16 GeV/c. (The subscripts are assigned for the purpose of labeling kinematic variables hereafter and B^- denotes missing mass with negative charge.) The square of the four-momentum transfer, u, equals $(p_1 - p_3)^2$, where p_i is the four-momentum of particle i.

The missing-mass method was used to look for

peaks in the B^- mass spectra, such peaks being indicative of the production of a two-body final state consisting of a proton and a boson resonance (B^-). By using this method, it was necessary only to measure the momenta and angles of the incident pion $\pi_{(1)}^-$ and the recoil proton $p_{(3)}$. Some mass spectra, which are plotted as a function of the square of the missing mass, $M^2 = (p_1 + p_2 - p_3)^2$, are shown in Figs. 1 and 2.

Since the apparatus has been described in detail elsewhere,[1] it will be described only briefly here. It consisted primarily of an incident-beam transport system and a recoil spectrometer. The incident beam contained Cherenkov counters for particle identification and scintillation hodoscopes for precise momentum ($\Delta P/P = \pm 0.25\%$) and angle ($\Delta\theta = \pm 0.8$ mrad) determination at high intensities (10^6 π^-/pulse). The recoil-particle spectrometer subtended a laboratory solid angle of 0.4 msr and had a momentum acceptance of $\Delta P/P = \pm 25\%$. A threshold Cherenkov counter situated at the end of this spectrometer separated the protons of interest from background π^+'s and K^+'s. The recoil spectrometer determined proton angles and momenta to an accuracy of ± 0.2 mrad and $\pm 0.25\%$, respectively. The large acceptance, high data rate, and excellent resolution of this spectrometer were achieved by using large digitized spark chambers as the detectors. The large momentum acceptance allowed us to record in a single setting entire spectra such as those in Figs. 1 and 2. The overall resolution in the square of the missing mass δM^2 was ± 0.075 GeV^2 and was constant over the M^2 range measured in this experiment.

Corrections to the raw data were: target-empty background (3%), muon contamination in the beam (3%), nuclear absorption in the target (13%) and in the recoil spectrometer (5%), and detection inefficiency (20%).

Data on reactions of the type

$$\pi^- p \to (\pi^+ \text{ or } K^+)(\text{missing mass}) \qquad (2)$$

in which a π^+ (or K^+) was detected were recorded simultaneously with the data in which a proton was detected. The smoothness of the missing-mass spectra measured when the detected particle was a π^+ (or K^+) along with detailed studies of the uniformity of response of the Cherenkov counter at the end of the recoil spectrometer provide solid evidence that there are no biases in the apparatus which could give rise to false peaks in the missing-mass spectra. The inefficiency of this Cherenkov counter in vetoing π^+

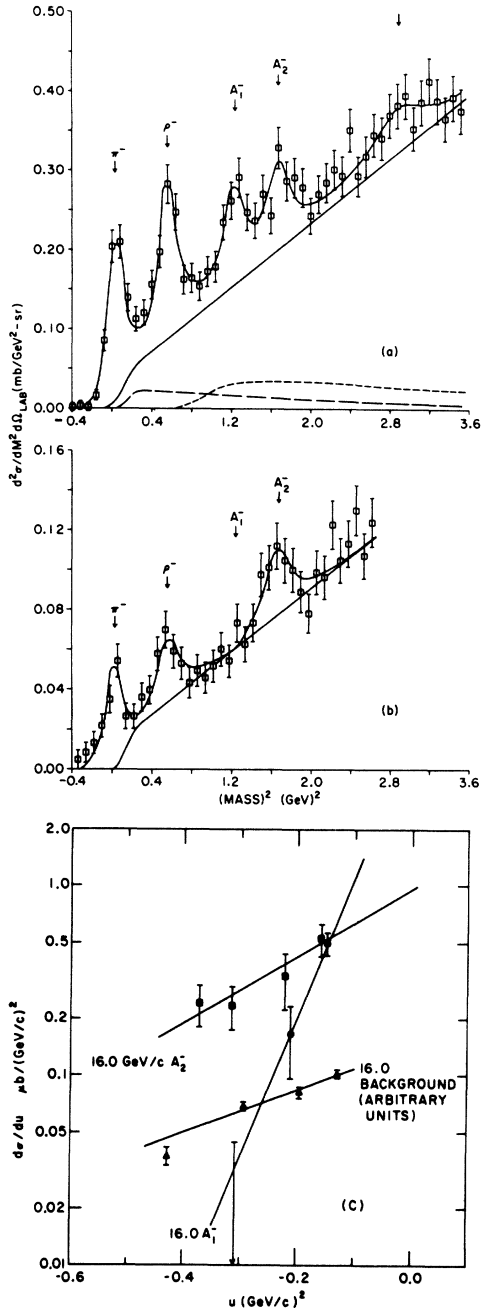

FIG. 1. (a) Missing-mass spectrum plotted versus M^2 for the reaction $\pi^- p \to pB^-$ for $M_{B^-} \leq 1.88$ GeV at an incident momenta of 16 GeV/c. The laboratory proton angles are $\theta_p = 20$-26 mrad. The short- and long-dashed lines are the results of Monte Carlo calculations described in the text. (b) Same as (a) but $\theta_p = 34$-50 mrad. The arrows in (a) and (b) are explained in the text. (c) $d\sigma/du$ for A_1^- and A_2^- production near 180° at 16 GeV/c. The values for the coefficients $a(u)$ (arbitrary units) are also given. The parameters of the fits to the cross sections of the form $A\exp(Bu)$ (plotted as solid lines) are given in Table I. In (a) and (b) the solid lines are the results of the least-squares fits described in the text.

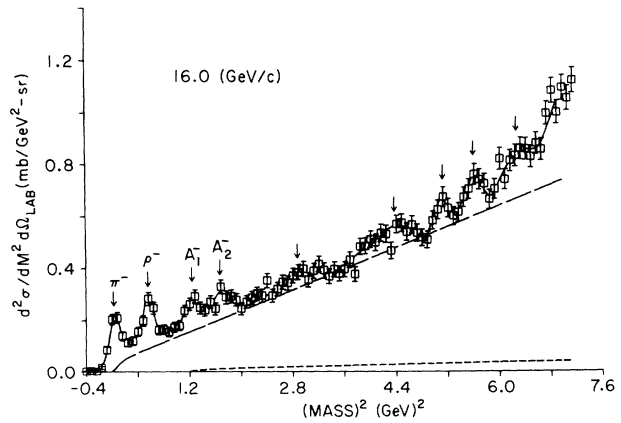

FIG. 2. Missing-mass spectrum for $\pi^- p \to pB^-$, $M_{B^-} \leq 2.66$ GeV, and $\theta_p = 20$-26 mrad. The lines and arrows are described in the text.

and K^+ resulted in a background which rises smoothly with M^2 and is less than 6% of the proton signal. This background is shown with the data in Fig. 2 (short-dashed line).

For $M_{B^-}{}^2 \leq 2.0$ GeV^2 the qualitative features of the data are as follows: At large proton laboratory angles [$34 \leq \theta_p \leq 50$ mrad, see Fig. 1(b)] well-defined peaks in the missing-mass spectra appear at the π^-, ρ^-, and A_2^- masses. However, in the small-angle data [$20 \leq \theta_p \leq 26$ mrad, Fig. 1(a)] an additional enhancement appears between the ρ^- and A_2^- peaks. This enhancement is consistent in mass and width with the A_1^- particle observed by others.[2] If the A_1^- enhancement seen in these data does, in fact, correspond to the controversial 3π resonance at this mass, then its observation here lends support to the resonance interpretation of the A_1^-.[3]

In order to extract differential cross sections from the missing-mass spectra, a least-squares fitting procedure was used. In these fits the spectra were assumed to be the sum of a Gaussian for the elastic peak (π^-), Breit-Wigner shapes for the resonances (ρ^-, A_1^-, A_2^-, and R^-), and an incoherent background. The best-fitting values for the masses, indicated by arrows in Figs. 1(a) and 1(b), and widths of the ρ^-, A_1^-, and A_2^- resonances are given in Table I. The parameters of the R used in the fits were $M_R = 1.700$ GeV and $\Gamma_R = 0.195$ GeV. For the background, shown as a solid line in Fig. 1(a), we have assumed the simplest form, namely $a(u)(M^2 - M_0{}^2)$, where $M_0{}^2$ was fixed at its best value of -0.36 GeV^2 and $a(u)$ was a free parameter of the fits.[4] The background behavior under and in the vicinity of the elastic peak was constrained by the elastic cross section and the known shape of the experimental resolution function. The results of these fits to data recorded at both 8.0- and 16.0-GeV/c beam momenta for $M^2 \leq 1.0$ GeV^2, from which π^- and ρ^- differential cross sections were extracted, are described in detail elsewhere.[1,5] The results of fits to the 16.0-GeV spectra which extend to $M^2 = 3.6$ GeV^2 are shown as solid lines through the data plotted in Figs. 1(a) and 1(b). The fit shown in Fig. 1(a) has a χ^2 probability of 25%, while a fit to the same data without the A_1^- enhancement has a χ^2 probability of 0.5%, thus confirming the statistical significance of the A_1^- enhancement.

In Fig. 1(c) we plot the resulting A_1^- and A_2^- differential cross sections and the background coefficients $a(u)$. The solid lines are fits of the form $A\exp(Bu)$ to the A_1^- and A_2^- cross sections $d\sigma/du$ and to the coefficients $a(u)$. The values

Table I. Values of the parameters A and B from fits to the cross sections of the form $d\sigma/du = A\exp(Bu)$ for $\pi^- p \to pB^-$ near 180° at 16 GeV/c, where $B^- = \pi^-, \rho^-, A_1^-, A_2^-$. The total backward cross sections are estimated as $\sigma = (A/B)\exp(Bu_{180°})$. The errors quoted below are explained in the text. The values for $B^- = \pi^-$ and ρ^- are taken from Refs. 1 and 5, respectively. The fits to the background parameter $a(u)$, evaluated in the laboratory system, are also given. In addition, the best-fit values for the ρ^-, A_1^-, and A_2^- masses are given.

B^-	A (μb/GeV/c^2)	B (GeV/c)$^{-2}$	σ (μb)	M_{B^-} (GeV)	Γ_{B^-} (GeV)
π^-	0.91 ± 0.13	4.23 ± 0.40	0.24 ± 0.03	0.140	
ρ^-	1.36 ± 0.21	4.44 ± 0.60	0.32 ± 0.04	0.750 ± 0.015	0.124 ± 0.015
A_1^-	$5.9^{+6.3}_{-4.2}$	16.9 ± 6.8	$0.35^{+0.87}_{-0.28}$	1.115 ± 0.020	$0.098^{+0.045}_{-0.020}$
A_2^-	0.95 ± 0.33	4.00 ± 1.32	0.21 ± 0.07	1.295 ± 0.020	$0.090^{+0.010}_{-0.050}$

Background: $A = 0.14 \pm 0.01$ mb/GeV^4 sr, $B = 2.6 \pm 0.3$ (GeV/c)$^{-2}$

for the parameters A and B are listed in Table I along with estimates of the total backward cross sections $\sigma_{tot} \simeq (A/B)\exp(Bu_{180°})$.

The errors on the data points in Fig. 1(c) and on the values of A, B, and σ in Table I are just those given by the least-squares fits to the spectra. We estimate that there is an additional uncertainty of ±50% in the overall normalization of the A_1^- and A_2^- results. This normalization uncertainty is mainly due to the uncertainty in the exact shape of the background under the peaks.

The A_1^- and A_2^- cross sections are, within errors, consistent with an exponential behavior in the u region studied. The fact that the cross sections as well as the background coefficients $a(u)$ vary smoothly with u indicate that the assumed shape for the background is a reasonable one.

It is noteworthy that the magnitudes of the total backward cross sections for pA_1^- and pA_2^- production are comparable with the backward $p\pi^-$ and $p\rho^-$ cross sections. However, in the small-u region, as in the small-t region,[6] the slope of the A_1^- cross section appears larger than the slopes of the π^-, ρ^-, and A_2^- cross sections. It is also of interest that the measured slopes and intercepts of the π^-, ρ^-, and A_2^- cross sections are approximately equal.

We have also examined our data recorded at 8 GeV/c for evidence of backward A_1^- and A_2^- production. In these 8-GeV/c data, the A_1^- and A_2^- are less apparent than in the 16-GeV/c data. Two possible reasons for this are the following: (1) The background in the A region arises from N^* decays (see text below). If this is the case, then one expects the signal-to-noise ratio to be significantly better at 16 than at 8 GeV/c. (2) The A_1^- and A_2^- backward cross sections fall less rapidly with energy than do the π^-, ρ^-, and background cross sections. The A_1^- and A_2^- peaks in the 8-GeV/c data each correspond to total backward cross sections of approximately $\sigma = 0.5^{+0.5}_{-0.3}$ μb, if one assumes that the angular dependence of the A_1^- and A_2^- cross sections is similar to that of the backward π^-p elastic cross section.

As a check that the peaks in the missing-mass spectra are indeed due to proton-plus-excited-pion final states we have performed Monte Carlo studies of reactions of the type

$$\pi^- p \to \pi N^* \\ \qquad\quad \lfloor \pi p,$$

where the N^* is produced near 0° in the c.m. system (i.e., at small u). Some results of these calculations, in the form of missing-mass spectra which would occur from events in which the N^* decay proton is detected, are shown as broken lines in Fig. 1(a). The short (long) dashed line shown in Fig. 1(a) is the calculated result for the N^* of mass 1238 (2190) MeV, width 120 (200) MeV, and $l_\pi = 1$ (3), where l_π is the orbital angular momenta in the N^* decay. In these calculations we assumed that the N^* is produced with 100% spin alignment, that the branching ratio for N^* into πp is 1, and that the N^* differential cross section is 4 times the known $\pi^- p$ backward elastic cross section at 16 GeV/c. Our complete studies, which included varying the N^* differential cross sections, clearly show that decay protons from excited baryons produced in two-body final states do not cause narrow peaks such as those apparent in our data.

In Fig. 2 we plot the missing-mass spectrum[7] for $0 \leq M^2 \leq 7.1$ GeV^2. The 20 000 events in this spectrum represent 6×10^{10} pions incident on the 3-ft-long hydrogen target or equivalently 45 h of AGS time. We present these data since they represent the first detailed search for high-mass bosons produced in the backward direction, and the data suggest there exist a number of excited pion states in the mass region 1.40-2.66 GeV. However, these bumps are of limited statistical significance.[8] In Fig. 2 the solid line is a smooth curve drawn through the data points. The long-dashed line representing the nonresonant background is an extrapolation of the linear background used in fitting the data shown in Fig. 1(a). The vertical arrows indicate the approximate location of the centers of the five high-mass ($M \geq 1.4$ GeV) enhancements evident in these data. The approximate masses and widths (M_i, Γ_i) of these enhancements in GeV are: (1.700 ± 0.047, 0.195), (2.086 ± 0.038, 0.150), (2.260 ± 0.018, ≤0.025), (2.370 ± 0.017, 0.057), and (2.500 ± 0.032, 0.087). These masses and widths can be compared with the R, S, T, and U peaks observed at small t by the CERN missing-mass spectrometer group[9] which have the following parameters: R (1.690 ± 0.015, 0.150), S (1.929 ± 0.014, <0.035), T (2.195 ± 0.015, <0.013), and U (2.382 ± 0.024, <0.030). It should be noted that peaks appear in our data at masses consistent with the R and U masses but not with the S and T masses. It is also interesting that both in our data (small u) and in the CERN data [$t \sim 0.2$ (GeV/c)^2] the peaks above 1.4 GeV appear as 10 to 20% effects above background and the ρ peak appears as a 100% effect in both cases. Thus for both forward and

backward production of charged bosons the signal-to-nonresonant background ratios are approximately the same.

It is a pleasure to acknowledge the generous cooperation and valuable assistance of the AGS staff in the setting up and running of this experiment. We also wish to acknowledge the important contributions made to this experiment by the staffs of the BNL On-Line Data Facility and Instrumentation Division (especially J. Fischer for design and construction of the wire chambers), and the Physics Design Groups at BNL and Carnegie-Mellon University. We are particularly grateful to A. Abrahamson, E. Bihn, R. Rothe, and J. Smith for their invaluable assistance throughout the experiment.

*Work performed under the auspices of the U. S. Atomic Energy Commission.

†Present address: National Accelerator Laboratory, Batavia, Ill.

‡Present address: Thomas J. Watson Research Center, IBM, Yorktown Heights, N. Y.

§Present address: The University of Birmingham, Birmingham 15, England.

[1]E. W. Anderson, E. J. Bleser, H. R. Blieden, G. B. Collins, D. Garelick, J. Menes, F. Turkot, D. Birnbaum, R. M. Edelstein, N. C. Hien, T. J. McMahon, J. Mucci, and J. Russ, Phys. Rev. Letters 20, 1529 (1968), and 21, 1030(E) (1968).

[2]Particle Data Group, University of California Radiation Laboratory Report No. UCRL 8030 (revised), 1968 (unpublished).

[3]C. C. Shih and B. L. Young (private communication) find that our A_1^- enhancement is not easily understood in terms of a simple backward multiperipheral calculation for the $p\rho\pi$ final state.

[4]We label the background coefficients $a(u)$ with the values of u calculated from the beam energy, the average laboratory angle of the data being fitted, and the ρ mass.

[5]E. W. Anderson, E. J. Bleser, H. R. Blieden, G. B. Collins, D. Garelick, J. Menes, F. Turkot, D. Birnbaum, R. M. Edelstein, N. C. Hien, T. J. McMahon, J. Mucci, and J. Russ, Phys. Rev. Letters 22, 102 (1969).

[6]M. Deutschmann et al., Phys. Letters 19, 608 (1965). The square of the four-momentum transfer $t = (p_1-p_4)^2$ in this experiment.

[7]For $M_{B^-}{}^2 < 3.6$ GeV^2 the data plotted in Fig. 1(a) are replotted in Fig. 2.

[8]We obtain χ^2 probability of approximately 5% when the high-mass ($2.0 \leq M^2 \leq 7.1$ GeV^2) data shown in Fig. 2 are fitted with a smooth structureless curve.

[9]J. Seguinot, M. Martin, B. Maglić, B. Levrat, F. Lefebvres, W. Kienzle, M. N. Focacci, L. Dubal, G. Chikovani, C. Bricman, H. R. Blieden, and P. Bareyre, Phys. Letters 19, 712 (1966); G. Chikovani, L. Dubal, M. N. Focacci, W. Kienzle, B. Levrat, B. Maglić, M. Martin, C. Nef, P. Schubelin, and J. Seguinot, Phys. Letters 22, 233 (1966).

STUDY OF THE PRODUCTION OF LOW-MASS $K^*\pi$ SYSTEMS IN 12.7-GeV/c K^+p COLLISIONS*

M. S. Farber, T. Ferbel, P. F. Slattery,† and H. Yuta
Department of Physics and Astronomy, University of Rochester, Rochester, New York
(Received 9 April 1969)

We have studied the production and decay characteristics of low-mass $K^{*0}(890)\pi^+$ systems produced in the reaction $K^+p \to K^+p\pi^+\pi^-$ at 12.7 GeV/c. Comparisons between these data and two diffractive production models are presented

We report on an investigation of the low-mass $K^+\pi^+\pi^-$ enhancement (Q bump) produced in the reaction[1]

$$K^+p \to K^+p\pi^+\pi^-. \quad (1)$$

This study is based on a 5-events/μb exposure of the Brookhaven National Laboratory 80-in. liquid-hydrogen bubble chamber to rf-separated 12.7-GeV/c K^+ mesons produced at the alternating-gradient synchroton.

The $K^+\pi^+\pi^-$ mass spectrum below 2 GeV/c in Reaction (1) consists predominately of $K^{*0}(890)\pi^+$ events.[2] In this note we compare the characteristics of this subset of Reaction (1) to the predictions of two diffractive models: (1) the particle exchange model of Ross and Yam (RY model),[3] which coherently sums the amplitudes for Feynman diagrams (A), (B), and (C) in Fig. 1; and (2) a double-Regge-exchange model[4] which considers just diagrams (B) and (C) (DR model).[5,6]

In the RY formulation we employed the usual parametrization of the three diagrams in Fig. 1.[7] No form factors were introduced at the dissociation vertices. The total cross sections σ (in mb) and the diffractive slopes β (in GeV^{-2}) which we used in our calculations are as follows: $\sigma_A = 18$ and $\beta_A = 7$ for diagram (A); $\sigma_B = 30$ and $\beta_B = 7$ for diagram (B); and, $\sigma_C = 18$ and $\beta_C = 5$ for diagram (C).